Spin Labeling Analysis of Structure and Dynamics of the Na^+/Proline Transporter of *Escherichia coli*†

Christoph Wegener,‡ Sandra Tebbe,§ Heinz-Jürgen Steinhoff,‡ and Heinrich Jung*,§

Universität Osnabrück, Fachbereich Biologie/Chemie, Arbeitsgruppe Mikrobiologie, Barbarastrasse 11, D-49069 Osnabrück, Germany, and Lehrstuhl für Biophysik, Ruhr-Universität Bochum, D-44780 Bochum, Germany

Received October 20, 1999; Revised Manuscript Received February 7, 2000

ABSTRACT: With respect to the functional importance attributed to the N-terminal part of the Na^+/proline transporter of *Escherichia coli* (PutP), we report here on the structural arrangement and functional dynamics of transmembrane domains (TMs) II and III and the adjoining loop regions. Information on membrane topography was obtained by analyzing the residual mobility of site-specifically-attached nitroxide spin label and by determination of collision frequencies of the nitroxide with oxygen and a polar metal ion complex using electron paramagnetic resonance (EPR) spectroscopy. The studies suggest that amino acids Phe45, Ser50, Ser54, Trp59, and Met62 are part of TM II while Gly39 and Arg40 are located at a membrane−water interface probably forming the cytoplasmic cap of the TM. Also Ala67 and Glu75 are at a membrane−water interface, suggesting a location close to the periplasmic ends of TMs II and III, respectively. Ser71 between these residues is clearly in a water-exposed loop (periplasmic loop 3). Spin labels attached to positions 80, 86, and 91 show EPR properties typical for a TM location (TM III). Leu97 may be part of a structured loop region while Ala107 is clearly located in a water-exposed loop (cytoplasmic loop 4). Finally, spin labels attached to the positions of Asp33 and Leu37 are clearly on the surface of the transporter and are directed into an apolar environment. These findings strongly support the recently proposed 13-helix model of PutP [Jung, H., Rübenhagen, R., Tebbe, S., Leifker, K., Tholema, N., Quick, M., and Schmid, R. (1998) *J. Biol. Chem. 273*, 26400−26407] and suggest that TMs II and III of the transporter are formed by amino acids Ser41 to Gly66 and Ser76 to Gly95, respectively. In addition to the topology analysis, it is shown that binding of Na^+ and/or proline to the transporter alters the mobility of the nitroxide group at the positions of Leu37 and Phe45. From these findings, it is concluded that binding of the ligands induces conformational alterations of PutP that involve at least parts of TM II and the preceding cytoplasmic loop.

The Na^+/solute symporter family (SSF)[1] currently comprises more than 40 proteins from archaea, bacteria, yeast, insects, and mammals (*1*, *2*). Substrates shown to be transported by members of this family are sugars, inositol, nucleosides, iodide, proline, pantothenate, and urea. While nothing is known about the tertiary structure of SSF proteins, information on the secondary structure of the polypeptide chains is improving. The average hydropathy plot for SSF proteins predicts 11−15 transmembrane domains (TMs) in α-helical conformation (*1*). Recent more precise analyses of the membrane topology of 3 members of this family, the human Na^+/glucose transporter (SGLT1), the thyroid Na^+/I^- symporter (NIS), and the Na^+/proline transporter (PutP) of *E. coli*, indicate a common topological motif of 13 transmembrane domains (*3*−*5*). According to these studies, the N-termini of the transporters are located on the outside of the membrane while the C-termini of NIS and PutP are directed into the cytoplasm. SGLT1 contains a C-terminal extension which is proposed to form an additional TM placing the C-terminus onto the outside of the membrane. Despite the general agreement of the secondary structure models of the three transporters, only little experimental evidence on the precise location of the TMs (i.e., TM boundaries) is available. By using PutP of *E. coli* as a model system, we are trying to improve the knowledge on the structures that underlie Na^+/solute symport.

PutP is an integral protein of the cytoplasmic membrane of *E. coli*. The transporter has been purified, reconstituted into proteoliposomes, and shown to be solely responsible for the coupled translocation of Na^+ and proline (*6*, *7*). Originally, PutP was proposed to consist of 12 TMs (*8*) (Figure 1A). In the recent 13-helix model, an additional TM is formed by amino acids of periplasmic loop 1 (pL 1) of the 12-helix motif (*5*) (Figure 1B). Evidence for this additional TM which forms putative TM II in the 13-helix

† This work was financially supported by the Deutsche Forschungsgemeinschaft SFB 394, C1 (H.-J.S.) and SFB 431, D4 (H.J.). H.J. received a postdoctoral fellowship from the Deutsche Forschungsgemeinschaft.

* To whom correspondence should be addressed at Universität Osnabrück, Fachbereich Biologie/Chemie, Mikrobiologie, Barbarastrasse 11, D-49069 Osnabrück, Germany. Tel: +49 541 9692276, Fax: +49 541 9692870, e-mail: jung_h@biologie.uni-osnabrueck.de.

‡ Ruhr-Universität Bochum.

§ Universität Osnabrück.

[1] Abbreviations: CROX, chromium oxalate; KP_i, potassium phosphate; cL, putative cytoplasmic loop; nitroxide spin label, (1-oxyl-2,2,5,5-tetramethylpyrroline-3-methyl)methanethiosulfonate; pL, putative periplasmic loop; SSF, sodium/solute symporter family; TM, putative transmembrane domain.

10.1021/bi992442x CCC: $19.00
Published on Web 03/31/2000

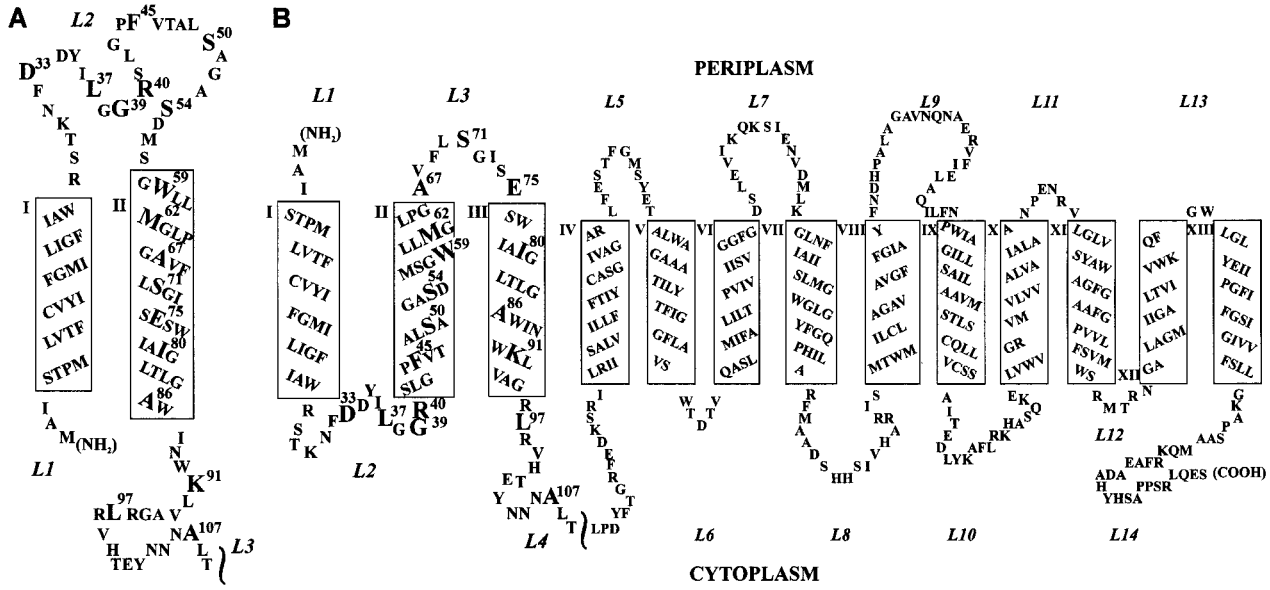

FIGURE 1: Secondary structure models of the Na^+/proline transporter of *E. coli*. (A) Topological arrangement of amino acids Met1 to Thr109 of PutP according to the 12-helix motif (*8*); (B) 13-helix secondary structure model of PutP [according to (*5*)]. Putative transmembrane domains are represented as rectangles and numbered with Roman numerals; loops are numbered with Arabic numerals starting from the N-terminus. Amino acid positions subjected to site-directed spin labeling are highlighted (boldface letters).

model comes from Cys accessibility and proteolysis studies. Remarkably, amino acids of this additional putative TM II proved to be of particular importance for transporter function. Thus, Asp55 is essential for transport activity and proposed to be involved in Na^+ binding (*9*). Furthermore, Ser57 is required for Na^+-dependent high-affinity binding of proline to PutP (*10*, *11*). Further substitution analyses indicate that Arg40 is important for the coupling of ion and proline transport and suggest a location close to the site of ion binding (*12*).

Because of the functional importance attributed to the N-terminal part of PutP, we have investigated the topological arrangement of amino acids comprising putative TMs II and III and the adjoining loop regions in more detail. In addition, the involvement of this region of the protein in ligand-induced conformational alterations has been tested. The studies are based on site-directed spin labeling of PutP and electron paramagnetic resonance (EPR) spectroscopy. The method of site-directed spin labeling has proven to be a powerful approach for the study of membrane protein structure and dynamics [for review see, e.g., (*13*−*15*)]. Site-specifically-placed Cys residues are used to introduce nitroxide radicals into specific sites within a protein sequence. EPR spectroscopy of the spin-labeled proteins yields structural information based on the mobility of the attached nitroxide, its accessibility to collisions with lipid- or water-soluble quenchers (*16*−*18*), and distance measurements between pairs of nitroxides through dipole−dipole interaction (*19*−*22*). The application of this method in the determination of local structures and molecular mechanisms of a variety of proteins has been very successful (*16*, *17*, *23*−*26*). Here we show that (i) TMs II and III of PutP are probably formed by amino acids Ser41 to Gly66 and Ser76 to Gly95, respectively, and (ii) Phe45 in TM II and Ile37 in the preceding cytoplasmic loop are involved in ligand-induced structural changes of the transporter.

EXPERIMENTAL PROCEDURES

Materials. Ni-NTA agarose was from Qiagen GmbH, Hilden, Germany. L-[^{14}C]Proline (261 μCi/μmol) was purchased from Amersham Buchler, Braunschweig, Germany. (1-Oxyl-2,2,5,5-tetramethylpyrroline-3-methyl)methanethiosulfonate (nitroxide spin label) was from Reanal, Budapest, Hungary. Gas-permeable TPX capillaries were from Jagmar Ltd., Kraków, Poland.

Mutagenesis, Expression, Purification, Spin Labeling, and Reconstitution of PutP. The generation of *putP* alleles encoding single Cys PutP molecules used in this study has already been described (*5*). For overexpression, the *putP* alleles were cloned into plasmid pTrc99a (*27*) using restriction endonucleases *Nco*I and *Hin*dIII. The resulting plasmids were transformed into *E. coli* WG170 (F$^-$ *trp lacZ rpsL thi* Δ*(putPA)101 proP219*) (*28*). Cells were grown, membranes were prepared, and PutP was solubilized and purified by Ni-NTA affinity chromatography as described (*7*). The eluted single Cys PutP molecules [in 50 mM KP_i, pH 8.0, containing 300 mM KCl, 200 mM imidazole, 10% glycerol (v/v), and 0.04% β-D-dodecylmaltoside (w/v)] were reacted with nitroxide spin label at a molar spin label-to-protein ratio of 10:1 at 4 °C for 3 h. Afterward, unbound label was removed by dialysis against 50 mM KP_i, pH 8.0, containing 10% glycerol and 0.04% β-D-dodecylmaltoside (w/v). The protein was reconstituted into proteoliposomes at a lipid-to-protein ratio of 20:1 (w/w) as described (*7*). Finally, the proteoliposomes were washed 2 times with 50 mM KP_i, pH 7.5, and resuspended in the same buffer to yield a PutP concentration of 30−80 μM. Proteoliposomes were frozen and stored in liquid N_2 until use.

Transport Measurements. The influence of amino acid substitutions on PutP activity was analyzed with intact cells of *E. coli* WG170 essentially as described previously (*9*). The activity of spin-labeled single Cys PutP derivatives reconstituted into proteoliposomes was determined in the

presence of an inwardly directed electrochemical Na^+ gradient as described (*7*).

EPR Measurements. EPR spectra were recorded with a homemade X-band EPR spectrometer equipped with a Bruker dielectric resonator or a homemade loop gap resonator (*29*). A Bruker B-NM 12 B-field meter was used to adjust the magnetic field. The PutP-proteoliposomes (5 μL) were loaded into EPR quartz capillaries. Spectra were taken at 293 K with a modulation amplitude of 1.5 G. After analogue to 12 bit digital conversion, the data were processed in a personal computer. As a measure of the nitroxide mobility, the peak−peak line width of the center line was determined after subtraction of the sharp components resulting from a small amount of unbound spin label.

For power saturation experiments in the presence of oxygen or chromium oxalate (CROX), the samples were loaded into gas-permeable TPX capillaries. The samples were deoxygenated by passing nitrogen around the sample capillary. For oxygen accessibility experiments, nitrogen was replaced by air. Saturation curves were determined from the peak−peak amplitudes of the center line measured at seven different incident microwave power levels in the range from 0.5 to 80 mW. The saturation behavior of the samples was parametrized by the quantity $P_{1/2}$, which is defined as the power level of the incident radiation at which the amplitude of the saturated line is half of the amplitude in the absence of saturation. Values for this parameter were calculated from fitting of the function:

$$A(P) = I\sqrt{P}[1 + (2^{1/\epsilon} - 1)P/P_{1/2}]^{-\epsilon}$$

to the experimental amplitudes $A(P)$ according to the method of (*30*). The scaling factor I and the measure of the saturation homogeneity ϵ are adjustable parameters. The quantity $\Delta P_{1/2}$ is calculated from the difference in $P_{1/2}$ values in the presence and absence of the relaxing agent. The $\Delta P_{1/2}$ values are divided by the peak−peak line width and normalized by the same quantity of a DPPH standard sample to obtain the dimensionless accessibility parameter Π.

RESULTS

Functional Properties of Spin-Labeled Single Cys PutP Molecules. Site-directed spin labeling of PutP was based on a functional transporter devoid of all five native Cys residues (Cys-free PutP) (*5*). As a prerequisite for the covalent attachment of spin label, amino acid residues in Cys-free PutP were individually replaced with Cys, and the effect of this alteration on transport was analyzed. As shown already in earlier studies, substitution of Asp33, Leu37, Phe45, Ser54, Ser71, Glu75, Ile80, and Lys91 in Cys-free PutP with Cys had no or only little effect on proline transport (*5*, *9*). Single Cys PutP-G39C,[2] -R40C, and -M62C exhibited initial rates of transport corresponding to 30−70% of the Cys-free PutP value while the proline uptake rate of PutP-S50C was about 10% of the Cys-free PutP value (*5*). In this study, Trp59, Ala67, Ala86, Leu97, and Ala107 of Cys-free PutP were individually substituted by Cys. The resulting transport proteins catalyzed proline accumulation to a steady-state level that was not significantly different from Cys-free PutP. Single Cys PutP-A86C, -L97C, and -A107C transported proline with more than 75% of the initial rate of Cys-free PutP. In the case of single Cys PutP-W59C and -A67C, the initial rate of transport was reduced to 26% and 46%, respectively, of the Cys-free transporter. Thus, all PutP derivatives tested showed a significant activity indicating that none of the substituted residues is essential for active transport.

Furthermore, the effect of site-directed spin labeling of PutP on transport activity was analyzed. Measurements were performed with proteoliposomes containing spin-labeled single Cys PutP derivatives or Cys-free PutP treated and prepared the same way as the other PutP derivatives. Active proline transport by single Cys PutP-K91C was not significantly affected by the reaction with MTS spin label. PutP-D33R1,[3] -F45R1, -I80R1, and -A107R1 catalyzed proline uptake at a rate corresponding to 30−40% of Cys-free PutP. Attachment of the spin label to a Cys at the position of Ser54, Ser71, Glu75, Ala86, or Leu97 reduced the proline uptake rate to 10−15% of the Cys-free PutP activity. Since the amino acid substitution itself had no or only very little effect on the transport activity of PutP, the reduced transport rates must be attributed to the labeling reaction. Finally, significant proline accumulation could not be detected for PutP-L37R1, -G39R1, -R40R1, -S50R1, -W59R1, -M62R1, and -A67R1.

EPR Spectra: Mobility of the Nitroxide Side Chains. All of the single Cys PutP derivatives reacted with the nitroxide spin label. The corresponding EPR spectra of the Na^+- and proline-free samples are shown in Figure 2 (solid lines), each revealing a unique spectral shape. Significant deviations of complete modification were observable for PutP-S54R1, -M62R1, and -L97R1. The variation of the signal-to-noise ratio for the other samples is mainly due to the different concentrations of sample loaded into the capillary.

Information of the protein structure in the vicinity of the spin label binding site is deduced from the mobility of the nitroxide side chain and the accessibility for polar and nonpolar paramagnetic reagents. The reorientational dynamics of the nitroxide side chain are constrained for residues with extensive tertiary contact interactions, as those oriented into the interior of the protein. For membrane proteins with very slow rotational diffusion, the EPR spectra of internal nitroxides approach those of powder spectra. This is obvious for the spectra of PutP-S54R1, -W59R1, -M62R1, -A67R1, -I80R1, -A86R1, -K91R1, and R97R1. Nitroxides attached to surface residues have a higher mobility. The apparent hyperfine splitting and the line width are decreased. Frequently, two components corresponding to different nitroxide mobilities are visible, as found for the spectra of PutP-D33R1, -L37R1, -G39R1, -R40R1, -F45R1, -S50R1, -S71R1, -E75R1, and -A107R1. A distribution of motional states can be concluded from these spectra. Additionally, the dynamics of the protein backbone may contribute to the mobility of the nitroxide to different extents (*18*). The information of

[2] Amino acid replacements are designated as follows: The one-letter amino acid code is used followed by a number indicating the position of the native residue in wild-type PutP. The sequence is followed by a second letter denoting the substitution at this position.

[3] Spin-labeled single Cys PutP derivatives are designated as follows: The one-letter amino acid code is used followed by a number indicating the position of the native residue in wild-type PutP. The sequence is followed by R1 representing the side chain generated by covalent modification of Cys at this position with the nitroxide spin label.

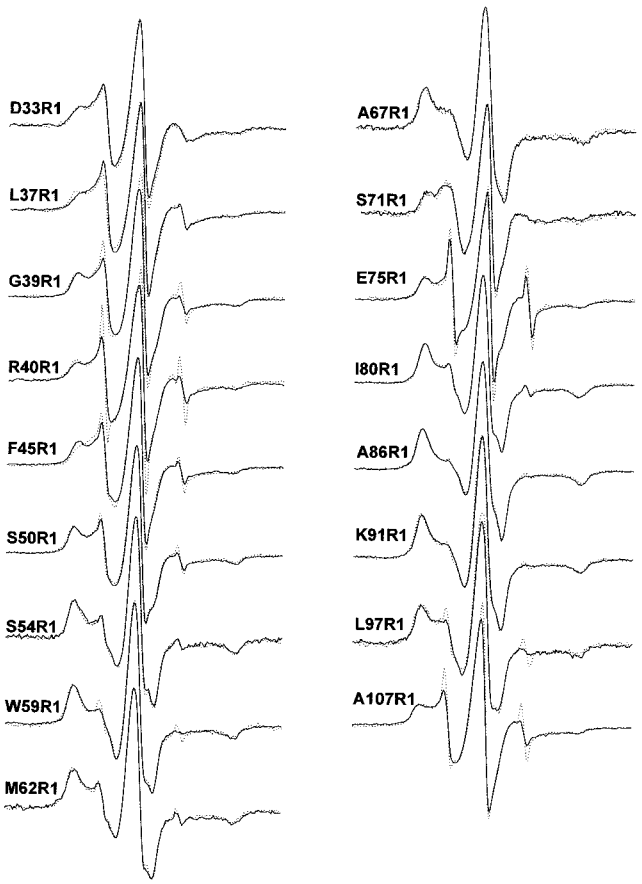

FIGURE 2: Room-temperature EPR spectra of the spin-labeled single Cys PutP derivatives in the absence (solid line) and in the presence of Na^+ and proline (dotted trace). Traces of different amounts of unbound spin labels (less than 2%) are responsible for the narrow lines visible in the spectra of PutP-G39R1, -R40R1, -F45R1, -E75R1, -L97C, and -A107R1. Due to the characteristic narrow line shape, their contribution can be easily separated from the signals of the bound spin labels and thus do not influence data analysis.

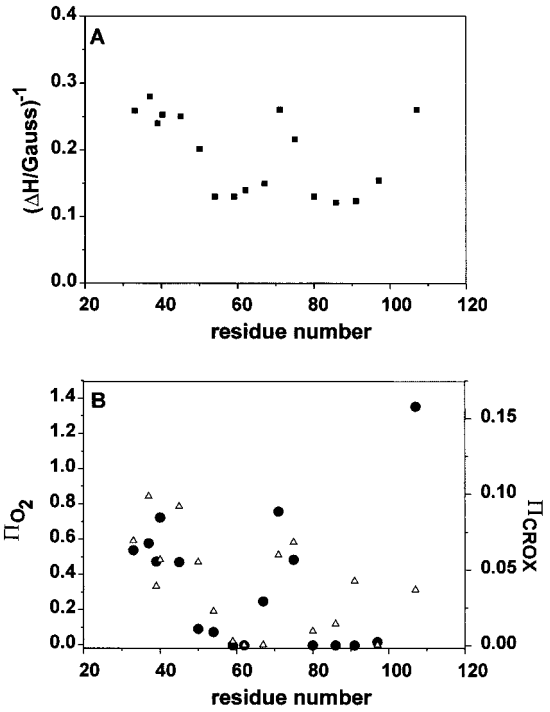

FIGURE 3: Mobility and accessibility of nitroxide groups covalently attached to PutP. (A) The reciprocal of the line width, ΔH^{-1}, is plotted versus the position of the spin label in the PutP sequence. The reciprocal of the line width is an estimator of the nitroxide dynamics and increases with increasing mobility. (B) The plot of the accessibility Π_{oxygen} (triangles) and Π_{CROX} (closed circles) versus the position of the nitroxide gives a view over the orientation of the spin-labeled side chains with respect to the protein, lipid, or aqueous phase (see text). Π_{oxygen} was measured in equilibrium with air and scaled to pure oxygen; Π_{CROX} was measured in the presence of 50 mM chromium oxalate.

the nitroxide dynamics can be extracted from the EPR line shape. A rigorous analysis requires spectral simulation techniques (*31*, *32*); however, for a simple graphical presentation, the reciprocal line width of the central resonance may be used as a crude parameter for the nitroxide dynamics. This parameter is shown in Figure 3A as a function of the sequence position. In the range from position 33 to position 45 and for positions 71, 75, and 107, the reciprocal line width exceeds the value of 0.2 G^{-1}, suggesting an exposed surface position of the nitroxide (*25*, *33*). The most mobile nitroxides with reciprocal line widths approaching 0.3 G^{-1} are found for spin labels bound at positions 33, 37, 71, and 107. These values are typical for exposed nitroxides located in interhelical loops (*25*, *33*). Most of these spectra show two components, and it has to be taken into account that the peak-to-peak line width is dominated by the most mobile component even though it is the minor one. However, the existence of the different components implies the environment is not globally restrictive, and the immobile state may arise from attractive interactions of the spin label with the immediate environment. In this picture, the conclusions drawn here are appropriate. A comparably low mobility is revealed for nitroxides in the sequence from positions 50 to 67 and from positions 75 to 97 with the reciprocal line widths less than 0.15 G^{-1}. Similar values were found for nitroxide side chains in regular structures in the hydrophobic domain of rhodopsin and bacteriorhodopsin (*25*, *33*).

Accessibilities to Oxygen and CROX. The accessibility parameter Π of the nitroxide side chains for freely diffusing paramagnetic quenchers was used to supplement the interpretation of the mobility data. The results are simple to interpret in terms of the local structure: the higher the density of neighboring residues around the nitroxide, the lower the accessibility. Molecular oxygen and water-soluble CROX have been found to be suited because of their sizes and solubility properties. Molecular oxygen has a low concentration in the tightly packed protein interior, whereas both the solubility and the diffusion coefficient are high in the bilayer. The collision frequency between spin labels and oxygen and therefore the accessibility parameter Π in the protein interior are low, whereas these are high if the spin label faces the bilayer. The negatively charged CROX is soluble in water but completely insoluble in the membrane and protein interior and, therefore, can be used to determine whether a side chain is exposed to water (*13*, *17*, *34*−*37*). However, one has to take into account that the collision frequency of the side chain with CROX is a function of both accessibility and local electrostatic potential. The latter parameter was reduced by the high salt concentration and, therefore, was not expected to be the determining parameter in the topology experiments.

The accessibility parameter in the presence of 50 mM CROX or with the sample in equilibrium with air was determined by the method of continuous wave power

saturation (*17*, *30*, *34*, *35*, *38*). The respective values are displayed in Figure 3B with the values of Π_{oxygen} scaled to pure oxygen. The highest values of Π_{CROX} and hence the highest collision frequency with CROX are found for the side chains attached to positions 40, 71, and 107. These residues must be oriented toward the aqueous phase. The ratio Π_{CROX}/Π_{oxygen} for PutP-R40R1 and -S71R1 is 0.17 ± 0.02, corresponding to a location for these nitroxides in the headgroup region of the lipid bilayer (*24*). The respective value for PutP-A107R1 yields 0.50 ± 0.05, consistent with the nitroxide located in the aqueous phase. The high accessibility of these residues for CROX is accompanied by high nitroxide mobilities (Figure 3A). A slightly lower accessibility for CROX is revealed for PutP-D33R1, -L37R1, -G39R1, -F45R1, and -E75R1. The ratio Π_{CROX}/Π_{oxygen} for these residues varies between 0.07 and 0.16, corresponding to a location of the nitroxides close to the headgroup region of the bilayer. Despite its low mobility, the nitroxide at position 67 is accessible for CROX with the ratio Π_{CROX}/Π_{oxygen} exceeding 0.5. This is evidence for this residue to be located close to or within the aqueous phase. The remaining residues with lower values of Π_{CROX} must face the protein or the bilayer, again in agreement with the mobility data. Residues at positions 50, 54, 80, 86, and 91 show Π_{CROX}/Π_{oxygen} ratios less than 0.05, consistent with a location in the membrane far from the water−lipid interface. All other residues are most likely oriented into the interior of the protein.

Structural Changes upon Binding of Na^+ and/or Proline. Most of the sites do not show any detectable changes in EPR spectral shape, and hence mobility, upon binding of Na^+ and proline (cf. Figure 2). However, significant changes of the line shape are observed for PutP-L37R1 and -F45R1. While the spectral change observed for nitroxide at position 37 represents an effective immobilization of the nitroxide, an effective mobilization is revealed for position 45. This can only arise from a change in tertiary interaction at these sites. A less significant increase of nitroxide mobility is observed for PutP-R40R1. To unravel whether Na^+ or proline or the combination of both induced the observed changes of tertiary interaction, EPR spectra of PutP-L37R1 and -F45R1 were recorded with either Na^+ or proline added to the respective mutant. The results are shown in Figure 4. The binding of Na^+ or proline reduces the mobility of residue L37C to a similar extent. However, the largest changes were observed with both substrates added simultaneously. A different picture results from inspection of the respective spectra of PutP-F45R1. The addition of Na^+ alone has virtually no effect on the mobility of the nitroxide, whereas the binding of proline results in a decrease of the mobility constraints. Further addition of Na^+ does not significantly alter the spectrum.

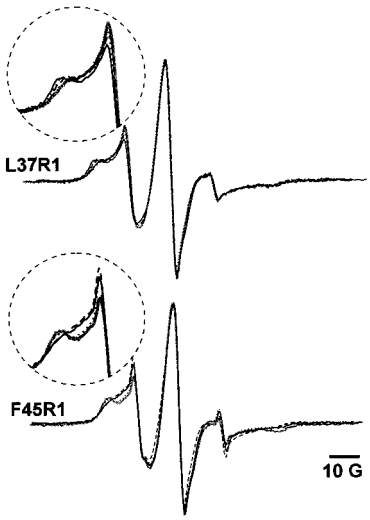

FIGURE 4: Influence of ligand binding on the EPR spectra of PutP-L37R1 and -F45R1. Spectral changes were observed upon addition of Na^+ (dotted trace) or proline (broken line). The spectra to the substrate-free samples (thick gray line) and after addition of both Na^+ and proline (solid line) are shown for comparison.

DISCUSSION

Site-directed spin labeling has been used to investigate membrane topology and functional dynamics of putative TMs II and III and adjoining loops of the Na^+/proline transporter of *E. coli*. As a prerequisite for these studies, a chemical reactive group, the sulfhydryl group, is introduced at defined positions in the primary structure of Cys-free PutP by individual replacement of amino acids with Cys. Most of the replacements have no or only little effect on PutP function [this study and (*5*)]. In this study, substitution only of Trp59 (TM II) and Ala67 (pL 3) by Cys is found to significantly reduce the initial rate of proline transport (26 and 46%, respectively, of Cys-free PutP) while the steady-state level of proline accumulation is not affected. These findings are in agreement with a variety of previous studies indicating that amino acids of TM II are particularly important for PutP function and may directly be involved in Na^+ binding (*9*−*12*). Importantly, all single Cys PutP derivatives used in this study catalyze significant active proline transport indicating a functional intact conformation.

With respect to the functional importance attributed to amino acids in TM II, it is not surprising that reaction of Cys at different positions in or close to TM II with the spin label inhibits active proline uptake to different extents. Clearly, introduction of the paramagnetic group into the transporter must introduce a local perturbation in structure. However, the molar volume of the spin label is only about 25% larger than a tryptophan side chain, and although the nitroxide group is hydrophobic, the nitroxide function can participate in hydrogen bonding and, therefore, the R1-labeled Cys is a reasonable compromise for the substitution of nonpolar as well as polar residues (*39*). Indeed, in multiple site-directed spin labeling studies with, for example, lysozyme, bacteriorhodopsin, rhodopsin, and lactose permease, the structural perturbation due to the introduction of the nitroxide is found to be small at the level of the backbone fold even for buried sites (*15*−*18*, *25*, *34*, *40*−*45*). Also in the case of PutP, introduction of the spin label into the protein most likely introduces only a local perturbation of protein structure rather than a general destruction. This assumption is supported by the following facts: (i) Reaction of single Cys PutP-L37C with the spin label blocks proline accumulation. However, binding of Na^+ and/or proline still induces a conformational alteration of the spin-labeled transporter (discussed below), indicating that the overall structure of PutP must at least be close to the native state. (ii) Chemical modification of Cys at the position of Arg40 inhibits proline accumulation completely but stimulates facilitated diffusion of proline (*12*).

Information on the topological organization of amino acids of TMs II and III and adjoining loops of PutP is obtained by analyzing the residual mobility of site-specifically-attached nitroxide side chains. The studies are complemented by determination of collision frequencies of the nitroxide with nonpolar oxygen and polar CROX. The results suggest that Gly39 and Arg40 are located in a water-exposed loop close to the membrane−water interface. The nitroxides at the positions of Phe45 and Ser50 show intermediate mobilities and are much more accessible to oxygen than to CROX (Π_{CROX}/Π_{oxygen} ratios of 0.08 and 0.05, respectively) and, therefore, are proposed to be in contact with the lipid bilayer. The nitroxide attached to position Ser54 is more buried within the protein. A Π_{CROX}/Π_{oxygen} ratio of less than 0.05 strongly supports a location of this residue within the membrane. The spin labels of PutP-W59R1 and -M62R1 are highly immobile and accessible neither to CROX nor to oxygen. These residues are obviously completely buried within the protein, and it cannot be discriminated between a location within the membrane or in a structured loop region. Nonetheless, the mobility parameters and accessibility values obtained for nitroxides attached to positions in the range of Phe45 and Met62 are very similar to those determined for nitroxides in TMs of rhodopsin and bacteriorhodopsin (*25*, *33*). These findings contradict a location of these positions in a loop region as suggested by the 12-helix model (Figure 1A) and favor the formation of an additional TM (TM II of the 13-helix model) (Figure 1B). Furthermore, the EPR data suggest that Ala67 and Glu75 are close to a membrane−water interface and, therefore, are most likely located at the periplasmic ends of TMs II and III, respectively. Ser71 between these residues is clearly in a water-exposed loop region. Also these results contradict the 12-helix model according to which Ser71 and Glu75 are located close to the middle of a TM (TM II of the 12-helix model) (Figure 1A). Instead, the data provide strong support for the idea that TM II is formed by amino acids Ser41 to Gly66. In addition, the borders of the following TM (TM III of the 13-helix model) are shifted by 8 amino acids toward the C-terminus, thereby moving Glu75 from the middle of the TM to its periplasmic end. In agreement with this conclusion, nitroxides attached to positions 80, 86, and 91 show EPR properties typical for a TM location (i.e., Π_{CROX}/Π_{oxygen} ratios less than 0.05) and are, therefore, thought to be part of TM III of the 13-helix model (Figure 1B). The restricted mobility and low accessibility of the nitroxide group attached to position 97 to both oxygen and CROX demonstrate that the spin label experiences tertiary interaction with other parts of the protein. The properties are similar to those described for nitroxide attached to the position of Met163 in the E-F loop of bacteriorhodopsin which is proposed to form a stretched turn (*25*). Nitroxide at the position of Ala107 is mobile and highly accessible from the aqueous phase and is clearly located in a water-exposed loop region. These findings are in good agreement with the recently proposed 13-helix model of PutP (*5*) (Figure 1B). Spin label attached to positions 33 and 37 shows mobility properties that are characteristic for a surface location. The relatively good accessibility to oxygen reveals that the paramagnetic group is in contact with the hydrophobic environment although previous Cys accessibility and site-specific proteolysis studies propose a location of Asp33 and Leu37 in a cytoplasmic loop (cL 2) (*5*). Most likely these amino acids are located close to the membrane surface, and nitroxide groups attached to these positions are directed into the apolar environment of the membrane. Similar observations were made for spin labels attached to positions 160 and 161 in the E-F loop of bacteriorhodopsin (*25*).

Taken together with studies on the topology of SGLT1 and the mammalian Na^+/I^- transporter (NIS), the results support the idea of a common topological motif for members of the SSF. Thus, the bacterial transporters for proline (PutP) and pantothenate (PanF) and the mammalian NIS are composed of 13 TMs (*2*). Transporters with a C-terminal extension [i.e., the human SGLT1 and myoinositol transporter (SMIT1)] are proposed to have an additional 14th TM (*2*, *3*).

Besides information on protein structure, knowledge of functional relevant conformational alterations of the transporter is another prerequisite for understanding Na^+-coupled solute transport at the molecular level. In our study, we utilize the sensitivity of nitroxide mobility to tertiary interactions as a means of detecting conformational movements of PutP. Analysis of EPR line shapes reveals ligand-induced mobility changes of nitroxide attached to positions 37 (cL 2) and 45 (TM II) of the transporter. In the case of single Cys PutP-L37C, binding of Na^+ and/or proline to the transporter leads to an immobilization of the spin label while the nitroxide at position 45 becomes more mobile upon addition of proline, and Na^+ alone has no effect. From these findings, it is concluded that proline binding induces a conformational alteration of PutP that involves at least parts of TM II and the preceding cytoplasmic loop. Na^+ could only be shown to affect the structure of cL 2.

The fact that changes in nitroxide mobility can only be observed at 2 out of 16 positions tested supports the idea that ligand binding affects only very selected parts of the transporter and are not global. However, it has to be taken into account that nitroxide mobility is not necessarily affected by a conformational alteration. Furthermore, local structural perturbations caused by chemical modification of a Cys in PutP may prevent structural changes. The latter idea is in agreement with the fact that spin labeling of PutP at a variety of positions inhibits active proline transport. Despite these limitations, the EPR studies confirm and extend previous investigations proposing an involvement of TM II and adjoining loops in ligand-induced conformational alterations. So, based on Cys accessibility analyses, Arg40 is shown to be important for the structural flexibility of the putative helix and thought to be involved in coupling downhill transport of Na^+ with the accumulation of proline (*12*). Furthermore, the accessibility of a Cys in place of Ser57 (TM II), Ser71 (pL 3), or Glu75 (pL 3) to sulfhydryl reagents is increased by Na^+, indicating a conformational alteration in this region of the protein induced by the coupling ion. For PutP-S57C, the Na^+ effect is partially reversed by addition of proline which might either be due to a structural change or be due to steric hindering (M. Langkamp, T. Pirch, and H. Jung, unpublished information). The nature of the structural alteration of PutP discussed here is still unclear. It can be speculated that binding of Na^+ and proline induces changes in helix tilt or helix rotation similar to that proposed for ligand-induced helix movements in the lactose permease of *E. coli* (LacY) (*46*−*48*).

In conclusion, by showing that TMs II and III of PutP are probably formed by amino acids Ser41 to Gly66 and Ser76 to Gly95, respectively, the studies presented here confirm and further specify the 13-helix model of PutP. Furthermore, it is demonstrated that binding of ligands induces conformational alterations of PutP that involve at least parts of TM II and the preceding cytoplasmic loop. In this way, experimental evidence is provided for the common idea that Na^+/solute symport is the result of conformational changes.

ACKNOWLEDGMENT

We thank Monika Nietschke for excellent technical assistance.

REFERENCES

1. Reizer, J., Reizer, A., and Saier, M. H. J. (1994) *Biochim. Biophys. Acta 1197*, 133−166.
2. Turk, E., and Wright, E. M. (1997) *J. Membr. Biol. 159*, 1−20.
3. Turk, E., Kerner, C. J., Lostao, M. P., and Wright, E. M. (1996) *J. Biol. Chem. 271*, 1925−1934.
4. Levy, O., De la Vieja, A., Ginter, C. S., Riedel, C., Dai, G., and Carrasco, N. (1998) *J. Biol. Chem. 273*, 22657−22663.
5. Jung, H., Rübenhagen, R., Tebbe, S., Leifker, K., Tholema, N., Quick, M., and Schmid, R. (1998) *J. Biol. Chem. 273*, 26400−26407.
6. Hanada, K., Yamato, I., and Anraku, Y. (1988) *J. Biol. Chem. 263*, 7181−7185.
7. Jung, H., Tebbe, S., Schmid, R., and Jung, K. (1998) *Biochemistry 37*, 11083−11088.
8. Nakao, T., Yamato, I., and Anraku, Y. (1987) *Mol. Gen. Genet. 208*, 70−75.
9. Quick, M., and Jung, H. (1997) *Biochemistry 36*, 4631−4636.
10. Jung, H. (1998) *Biochim. Biophys. Acta 1365*, 60−64.
11. Quick, M., Tebbe, S., and Jung, H. (1996) *Eur. J. Biochem. 239*, 732−736.
12. Quick, M., Stolting, S., and Jung, H. (1999) *Biochemistry 38*, 13523−13529.
13. Millhauser, G. L. (1992) *Trends Biochem. Sci. 17*, 448−452.
14. Hubbell, W. L., Mchaourab, H. S., Altenbach, C., and Lietzow, M. A. (1996) *Structure 4*, 779−783.
15. Hubbell, W. L., Gross, A., Langen, R., and Lietzow, M. A. (1998) *Curr. Opin. Struct. Biol. 8*, 649−656.
16. Altenbach, C., Cai, K., Khorana, H. G., and Hubbell, W. L. (1999) *Biochemistry 38*, 7931−7937.
17. Altenbach, C., Marti, T., Khorana, H. G., and Hubbell, W. L. (1990) *Science 248*, 1088−1092.
18. Mchaourab, H. S., Lietzow, M. A., Hideg, K., and Hubbell, W. L. (1996) *Biochemistry 35*, 7692−7704.
19. Rabenstein, M. D., and Shin, Y. K. (1995) *Proc. Natl. Acad. Sci. U.S.A. 92*, 8239−8243.
20. Steinhoff, H. J., Radzwill, N., Thevis, W., Lenz, V., Brandenburg, D., Antson, A., Dodson, G., and Wollmer, A. (1997) *Biophys. J. 73*, 3287−3298.
21. Mchaourab, H. S., Oh, K. J., Fang, C. J., and Hubbell, W. L. (1997) *Biochemistry 36*, 307−316.
22. Hustedt, E. J., Smirnov, A. I., Laub, C. F., Cobb, C. E., and Beth, A. H. (1997) *Biophys. J. 72*, 1861−1877.
23. Farrens, D. L., Altenbach, C., Yang, K., Hubbell, W. L., and Khorana, H. G. (1996) *Science 274*, 768−770.
24. Perozo, E., Cortes, D. M., and Cuello, L. G. (1998) *Nat. Struct. Biol. 5*, 459−469.
25. Pfeiffer, M., Rink, T., Gerwert, K., Oesterhelt, D., and Steinhoff, H. J. (1999) *J. Mol. Biol. 287*, 163−171.
26. Tiebel, B., Radzwill, N., Aung-Hilbrich, L. M., Helbl, V., Steinhoff, H. J., and Hillen, W. (1999) *J. Mol. Biol. 290*, 229−240.
27. Amann, E., Ochs, B., and Abel, K. J. (1988) *Gene 69*, 301−315.
28. Stalmach, M. E., Grothe, S., and Wood, J. M. (1983) *J. Bacteriol. 156*, 481−486.
29. Hubbell, W. L., Froncisz, W., and Hyde, J. S. (1987) *Rev. Sci. Instrum. 58*, 1879−1886.
30. Altenbach, C., Greenhalgh, D. A., Khorana, H. G., and Hubbell, W. L. (1994) *Proc. Natl. Acad. Sci. U.S.A. 91*, 1667−1671.
31. Schneider, D. J., and Freed, J. H. (1989) in *Biological Magnetic Resonance, Spin Labeling, Theory and Application* (Berliner, L. J., and Reuben, J., Eds.) pp 1−76, Plenum Press, New York.
32. Steinhoff, H. J., and Hubbell, W. L. (1996) *Biophys. J. 71*, 2201−2212.
33. Altenbach, C., Yang, K., Farrens, D. L., Farahbakhsh, Z. T., Khorana, H. G., and Hubbell, W. L. (1996) *Biochemistry 35*, 12470−12478.
34. Altenbach, C., Flitsch, S. L., Khorana, H. G., and Hubbell, W. L. (1989) *Biochemistry 28*, 7806−7812.
35. Altenbach, C., Froncisz, W., Hyde, J. S., and Hubbell, W. L. (1989) *Biophys. J. 56*, 1183−1191.
36. Zhao, M., Zen, K. C., Hernandez-Borrell, J., Altenbach, C., Hubbell, W. L., and Kaback, H. R. (1999) *Biochemistry 38*, 15970−15977.
37. Liu, J., Rutz, J. M., Klebba, P. E., and Feix, J. B. (1994) *Biochemistry 33*, 13274−13283.
38. Poole, C. P. (1983) *Electron Spin Resonance*, Wiley, New York.
39. Hubbell, W. L., and Altenbach, C. (1994) *Curr. Opin. Struct. Biol. 4*, 566−573.
40. Steinhoff, H. J., Mollaaghababa, R., Altenbach, C., Hideg, K., Krebs, M., Khorana, H. G., and Hubbell, W. L. (1994) *Science 266*, 105−107.
41. Steinhoff, H. J., and Schwemer, J. (1996) *J. Photochem. Photobiol. B 35*, 1−6.
42. He, M. M., Voss, J., Hubbell, W. L., and Kaback, H. R. (1997) *Biochemistry 36*, 13682−13687.
43. Voss, J., He, M. M., Hubbell, W. L., and Kaback, H. R. (1996) *Biochemistry 35*, 12915−12918.
44. Voss, J., Hubbell, W. L., Hernandez-Borrell, J., and Kaback, H. R. (1997) *Biochemistry 36*, 15055−15061.
45. Voss, J., Hubbell, W. L., and Kaback, H. R. (1998) *Biochemistry 37*, 211−216.
46. Wu, J., Hardy, D., and Kaback, H. R. (1998) *Biochemistry 37*, 15785−15790.
47. Wu, J., Hardy, D., and Kaback, H. R. (1998) *J. Mol. Biol. 282*, 959−967.
48. Frillingos, S., Sahin-Toth, M., Wu, J., and Kaback, H. R. (1998) *FASEB J. 12*, 1281−1299.

BI992442X